

Triple-Shock Configurations, Vortices, and Instabilities Resulting from the Interaction of Energy Release with a Shock Layer in Gaseous Media

O. A. Azarova and L. G. Gvozdeva

Abstract Triple-shock configurations and vortex structures are researched in problems of control of a high-speed flow past an aerodynamic body “plate-cylinder” at freestream Mach number $M = 4$. The effect of an energy source dislocated in the incoming flow ahead of a bow shock is evaluated for the gaseous media of different physical–chemical properties in a range of the ratio of specific heats γ from 1.1 to 1.4. The energy source is modeled as a heated rarefied channel. Changing the angles in triple-shock configuration and the effect of the stagnation pressure decreasing together with the front drag force reduction is studied depending on γ and rarefaction factor in the energy source. Generation of the Richtmyer–Meshkov instability accompanied the forming of the triple configuration is modeled for $M = 8$. Complex conservative difference schemes are used in the simulations.

1 Introduction

Triple-shock configurations together with vortex structures constitute the basic elements of supersonic aerodynamics both the external and internal ones. These configurations define the distribution of the dynamics and heat stresses on flight vehicles, thrust and efficiency of rocket engines. Investigations of such types of structures appear as a fundamental problem in supersonic aerodynamics. In aerospace high-velocity engineering, it is necessary to consider physical–chemical reactions which are taken place behind the shock waves fronts and lead to the decreasing of the ratio of the specific heats γ there.

O. A. Azarova

A. A. Dorodnicyn Computing Centre of Federal Research Center “Computer Sciences, and Control” RAS, Vavilova Str. 40, 119333 Moscow, Russia

L. G. Gvozdeva (✉)

Joint Institute for High Temperatures RAS, Izhorskaya Str. 13/2, 125412 Moscow, Russia
e-mail: gvozdevalg@mail.ru

The effect of γ on triple configurations in the processes of unsteady reflection has been studied in Bazhenova et al. [1]. Theoretical investigations of the specific heats ratio γ effect on the particular features of shock waves reflection were conducted in Arutyunyan et al. [2]. In Gvozdeva et al. [3], it has been shown that the factor γ effects essentially not only on the dislocation of the shock waves in a triple configuration but on the share layers generating in the unsteady triple configurations. Essential effect of the specific heats ratio γ on triple-shock wave structures in a steady flow has been shown in Gvozdeva and Gavrenkov [4].

The triple configurations accompanied by the vortices generation have been obtained in problems of flow control via external energy supply (e.g., see Georgievsky and Levin [5], Azarova [6], Azarova et al. [7]). Supersonic flows with the Mach number of the incoming flow M in the range 1.89–3 and $\gamma = 1.4$ have been considered. Extensive reviews on the problems of flow control via external energy supply are presented in Knight [8, 9] and Russell et al. [10].

The research of the effect of physical–chemical transformations in a wide range of the values of γ on the dynamics of unsteady triple-shock configurations and vortex structures arising in the problems of supersonic streamlining with external energy sources in gaseous media is the objective of this chapter. The approach has been suggested in Azarova and Gvozdeva [11] where together with the angles of triple configurations the stagnation pressure and frontal drag force were studied for different γ .

In this chapter, the connection of the dynamics of triple-shock configurations with the defining flow parameters has been considered for $M = 4$, γ from 1.1 to 1.4 and different energy source characteristics. For $M = 8$ and $\gamma = 1.3$, the generation of the Richtmyer–Meshkov instability has been modeled. The obtained results may be useful for the developing the techniques of supersonic flow control via micro-wave and laser energy deposition.

2 Statement of Problem and Methodology

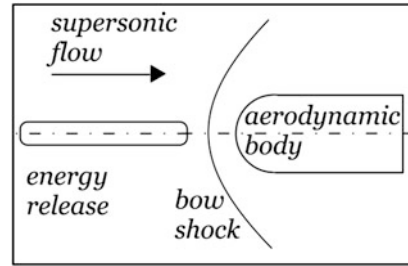
The modeling is based on the Euler equations for an ideal gas with the constant ratio of specific heats γ in the range from 1.1 to 1.4:

$$\frac{\partial \mathbf{U}}{\partial t} + \frac{\partial \mathbf{F}}{\partial x} + \frac{\partial \mathbf{G}}{\partial y} = \mathbf{H}, \quad (1)$$

$$\mathbf{U} = \begin{pmatrix} \rho \\ \rho u \\ \rho v \\ E \end{pmatrix}, \quad \mathbf{F} = \begin{pmatrix} \rho u \\ p + \rho u^2 \\ \rho uv \\ u(E + p) \end{pmatrix}, \quad \mathbf{G} = \begin{pmatrix} \rho v \\ \rho uv \\ p + \rho v^2 \\ v(E + p) \end{pmatrix}, \quad \mathbf{H} = \begin{pmatrix} 0 \\ 0 \\ 0 \\ 0 \end{pmatrix}.$$

Here ρ , p —density and pressure of the gas, u and v are x - and y - components of the gas velocity, $\varepsilon = p/\rho(\gamma-1)$, $E_S = \rho(\varepsilon + 0.5(u^2 + v^2))$ is the total energy per unit

Fig. 1 Flow configuration (schematic)



volume, ε is the specific internal energy. The schematic of the statement of the problem of supersonic flow control using an external energy source is presented in Fig. 1. Initial condition for the problem is a converged supersonic steady flow streamlining an aerodynamic body “a plate blunted by a cylinder”. Nondimensional freestream parameters are $\rho_\infty = 1$, $p_\infty = 0.2$, $u_\infty = Mc_\infty$, $v_\infty = 0$ (c_∞ is the undisturbed sound speed). For normalizing parameters for density 1.293 kg/m^3 and pressure $5.06625 \times 10^5 \text{ Pa}$, the dimensional freestream values of density and pressure correspond to those of air under the normal conditions. In Sects. 3.1–3.4 the freestream Mach number M is equal to 4, and in Sect. 3.5 $M = 8$.

The energy release is supposed to arise instantly ahead of the bow shock wave at a time moment t_i . The energy source is modeled as a heated rarefied homogeneous channel (layer). This model of the energy release was suggested in Artem’ev et al. [12]. Density in this channel is set as $\rho_i = \alpha_\rho \rho_\infty$, i.e., $\alpha_\rho = \rho_i / \rho_\infty$ is a rarefaction factor of the gas in the energy source. Other parameters inside the energy release area are set equal to the parameters of the oncoming flow.

Complex conservative difference schemes of the second approximation order are used in the simulations (see Azarova [13]). The schemes are a subset of the minimum stencil schemes (see Grudnitsky and Prohorchuk [14] and Belotserkovsky et al. [15]) with enlarged conservation properties which are based on the divergence forms for the systems of differential consequences for space derivatives (see Azarova [19]). The staggered Cartesian difference grids with the equal space steps, $h_x = h_y$, and 1000 nodes per the body’s diameter are used.

3 Results

3.1 Generation of a Triple Configuration

It has been stated that the triple configuration accompanied by the vortex structure was generated at the beginning stage of the process of the energy release—shock layer interaction (Fig. 2). The very beginning of the generation of the triple configuration is shown in Fig. 3. It can be seen that in the process of forming triple configuration the second triple point is originating on the bow shock (Fig. 3a). This

situation resembles the arising of the second triple point on the Mach wave in a problem of unsteady reflection of a shock wave of the wedge surface. The appearance of this point was obtained experimentally in Semenov et al. [16] and explained physically in Bazhenova et al. [17]. Numerically the effect of arising the second triple point on the Mach wave was found in Gvozdeva et al. [18].

Fig. 2 Dynamics of the triple-shock configuration initiated by energy release—shock layer interaction, fields of density: $M = 4$, $\gamma = 1.1$, $\alpha_p = 0.5$, $t_i = 0.601$; **a** nondimensional time $t = 0.68$, **b** $t = 0.72$, **c** $t = 0.76$, **d** $t = 0.8$

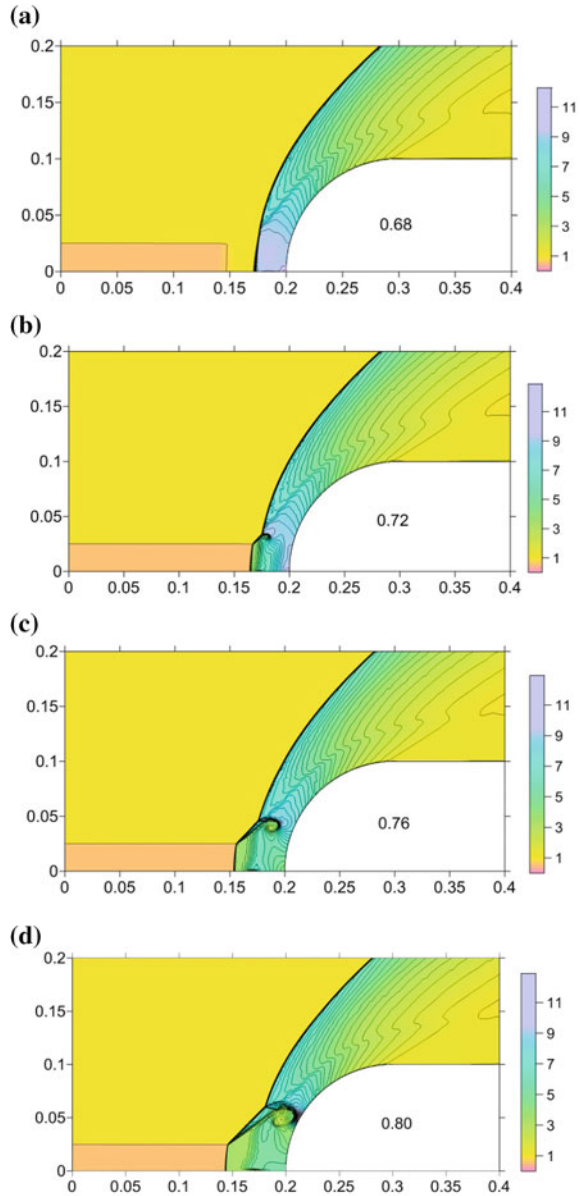


Fig. 3 Dynamics of the very beginning of generation of a triple configuration, fields of density: $M = 4$, $\gamma = 1.1$, $\alpha_p = 0.65$, $t_i = 0.501$; **a** nondimensional time $t = 0.57$, **b** $t = 0.59$, **c** $t = 0.61$

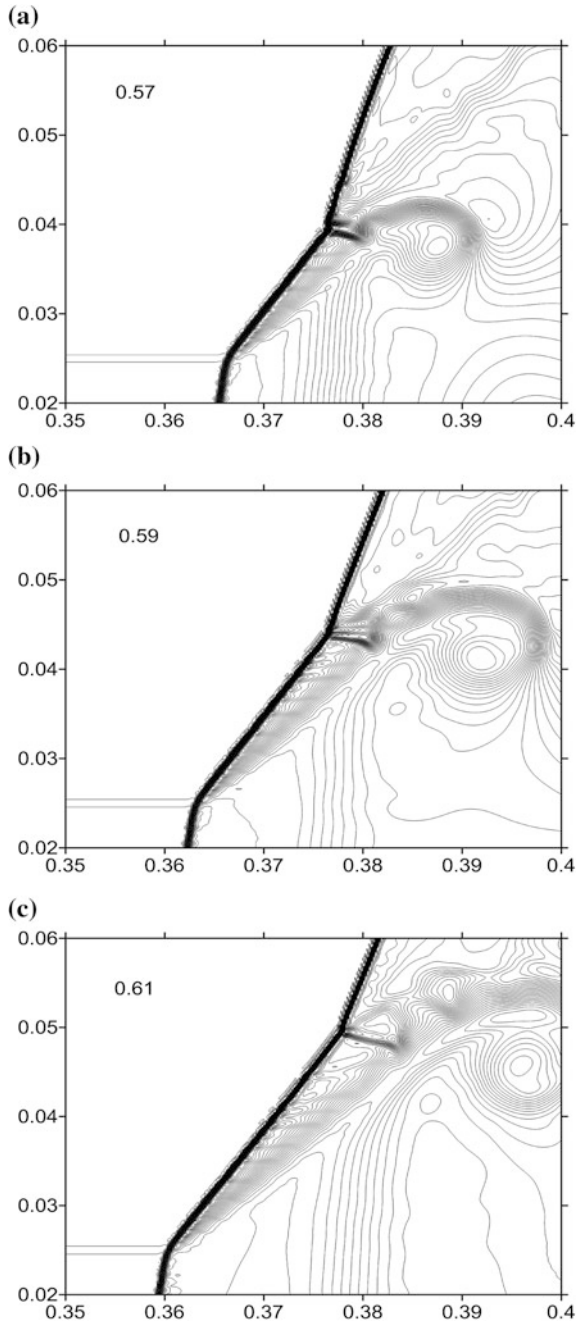
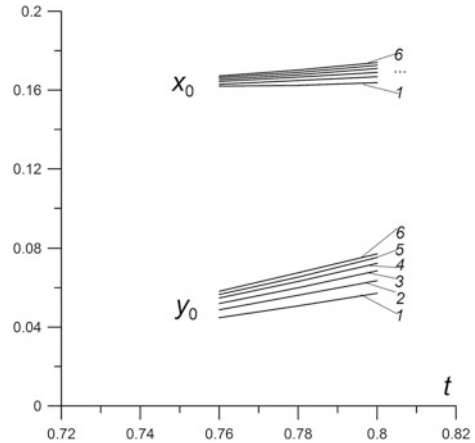


Fig. 4 Dynamics of the coordinates of the centers of triple configurations, $M = 4$, $\gamma = 1.2$: curve 1— $\alpha_p = 0.59$, curve 2— $\alpha_p = 0.50$, curve 3— $\alpha_p = 0.41$, curve 4— $\alpha_p = 0.33$, curve 5— $\alpha_p = 0.25$, curve 6— $\alpha_p = 0.18$



From some time moment the type of the developing of the triple configuration is close to a self-similar one, i.e., the angles in it are changing negligibly (Fig. 2c, d). Actually, in Fig. 4 the dynamics of the coordinates of centers of triple configurations are presented for different α_p which are seen to be the straight lines. Thus, Fig. 4 confirms the self-similar character of the considered processes. It allows us to study the angles forming the triple configuration using the three shock theory.

3.2 Analysis of Triple Configurations for Different γ

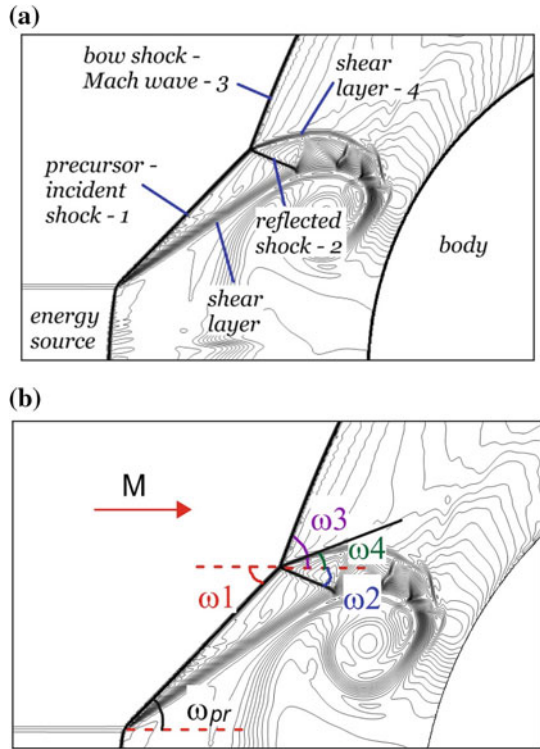
The scheme of the flow in the area of the triple configuration applying to the three shock theory and the researched angles can be seen in Fig. 5. The triple configurations for different γ are presented in Fig. 6.

Let us study the angles with the direction of the oncoming flow of the elements of the triple configuration: ω_1 —the angle of the incident shock wave (1), ω_2 —the angle of the reflected shock wave (2), ω_3 —the angle of the Mach wave (3) and ω_4 —the angle of the contact discontinuity (shear layer) (4) (see Fig. 5). Indeed, the angle ω_4 is the angle of the flow deflection by the Mach shock in the stationary system of coordinates connected with the center of the triple configuration (defined as θ_3 in Gvozdeva and Gavrenkov [4]).

Dependences of these angles on γ for $\alpha_p = 0.5$ have been obtained earlier in Azarova, Gvozdeva [11] (Fig. 7). The angles were estimated via the coordinates on the shock fronts. These fronts are not precisely straight lines, so the coordinates have been chosen in the areas in which the fronts were the closest to the linear ones.

One can see that the angle formed by the reflected shock ω_2 is changing significantly with γ decreasing from 1.4 to 1.1 (by 51.8%), the angle of the Mach wave ω_3 is changing not so strongly (by 11.5%) and the angles ω_1 and ω_4 are practically

Fig. 5 Scheme of the triple-shock configuration (a); considered angles (b)



independent of γ . In Table 1, the values of these angles are collected for γ decreasing from 1.4 to 1.1.

It is established that the angle ω_1 is quite well approximated (about 3% for moderate α_p) by the relation:

$$\sin^2 \omega_{pr} = \alpha_p \tag{2}$$

which was obtained in Artem'ev et al. [12] for the precursor angle ω_{pr} (Fig. 8). So ω_1 increases against α_p . In its turn, the calculations have shown that the precursor angle is excellently described by (2) for γ from 1.4 to 1.1 (with the deviation about 0.3–0.4% for moderate α_p) and is independent of γ .

The behavior of the other considered angles for α_p changing in the interval (0.11; 0.66) for different γ is presented in Figs. 9 and 10. It is obtained that for all γ the angle of the reflected shock ω_2 has the local minimum in the interval $0.11 < \alpha_p < 0.66$, the angle of the Mach shock ω_3 decreases slightly against α_p and the angle of the contact discontinuity ω_4 increases against α_p . At the same time ω_2 decreases with decreasing γ , ω_3 slightly increases with decreasing γ and the dependence on γ is not shown in the behavior of ω_4 .

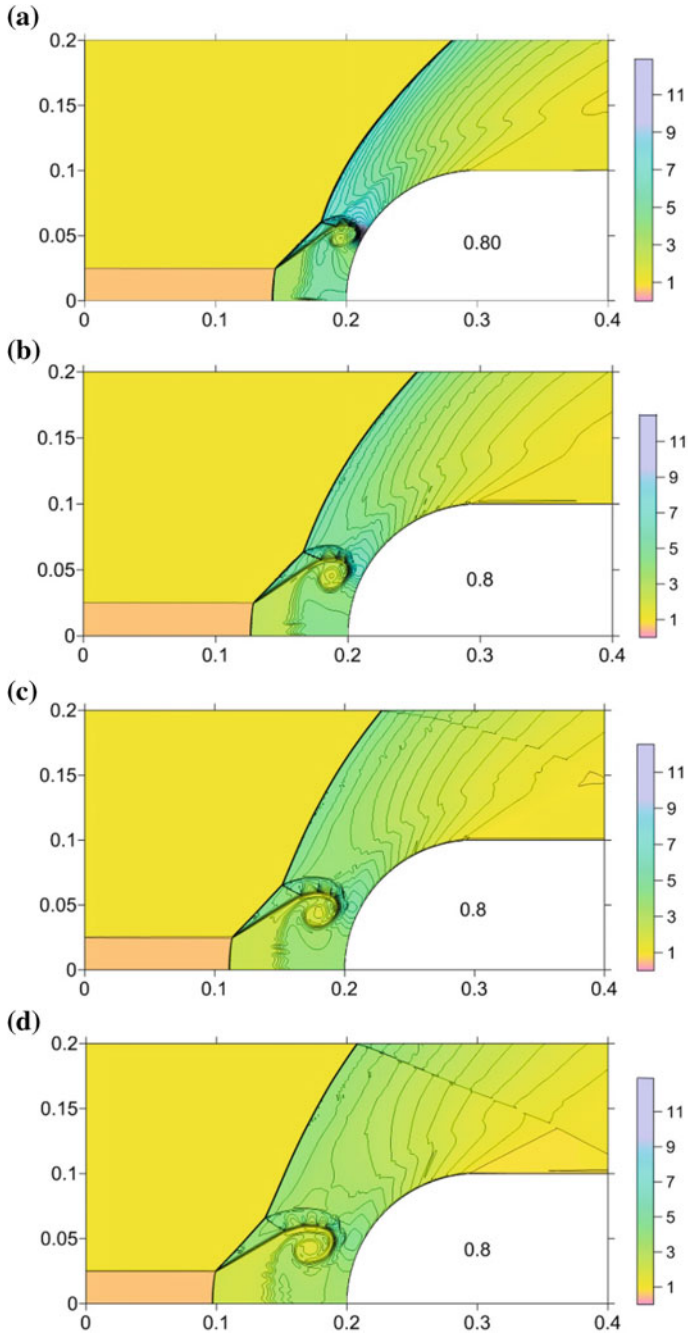


Fig. 6 Triple-shock configurations for different γ , fields of density, $M = 4$, $t = 0.8$, $\alpha_p = 0.5$, $t_i = 0.601$: **a** $\gamma = 1.1$, **b** $\gamma = 1.2$ (Azarova and Gvozdeva [11]), **c** $\gamma = 1.3$, **d** $\gamma = 1.4$

Fig. 7 Dependences of the angles in triple configurations on γ , $M = 4$, $\alpha_p = 0.5$ from Azarova and Gvozdeva [11]

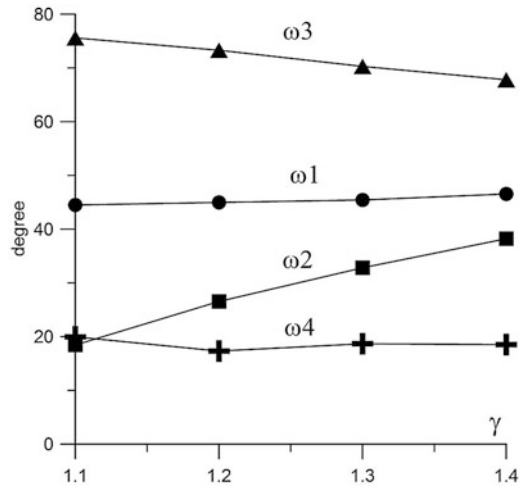


Table 1 Analysis of changing the angles in the triple-shock configurations for γ decreasing from 1.4 to 1.1

Angle	Related changing: $\text{abs}[(\omega(1.4) - \omega_{\min}(\gamma))/\omega(1.4)]$ (%)	Character of changing with decreasing γ
ω_1	4.5	practically independent of γ
ω_2	51.8	decreases
ω_3	11.5	increases
ω_4	6.8	practically independent of γ

Fig. 8 Dependence of the angle ω_1 (solid lines) and ω_{pr} (dashed line) on α_p for different γ , $M = 4$

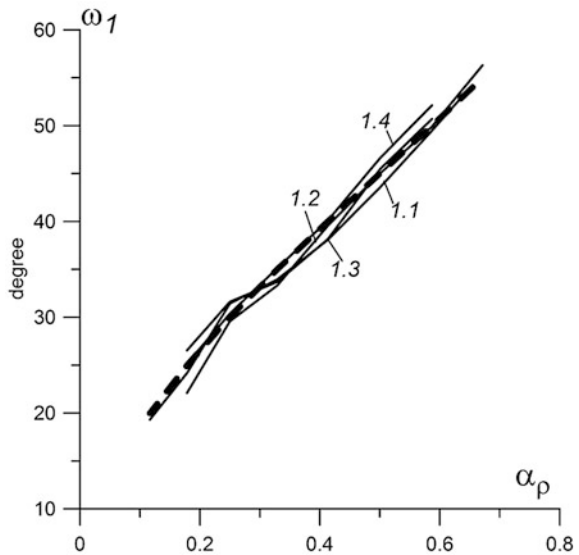


Fig. 9 Dependence of the angle ω_2 on α_p for different γ , $M = 4$

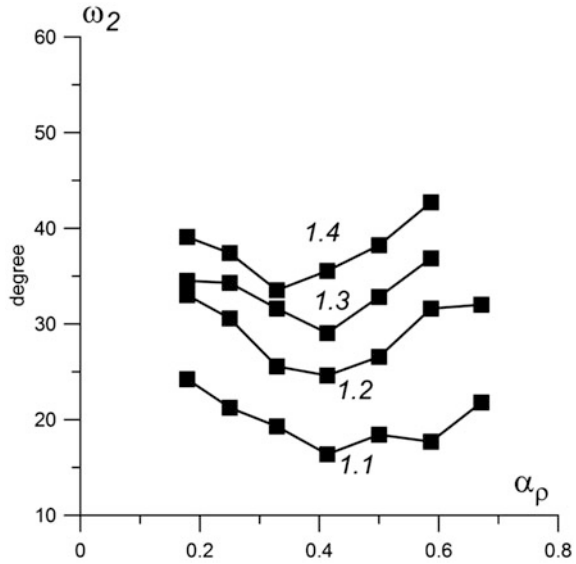
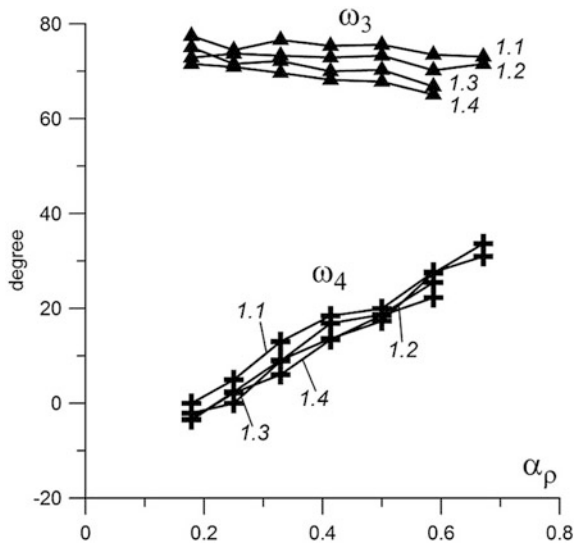


Fig. 10 Dependences of the angles ω_3 and ω_4 on α_p for different γ , $M = 4$



3.3 Accuracy of the Angles Calculations

The scheme accuracy of the shock fronts in the calculations constitutes tenth parts of a percent. Basically, a total accuracy of a triple configuration angles evaluation for the flow mode close to the self-similar one is connected with the accuracy of the angles calculations using flow images. We have used the enlarged flow images and

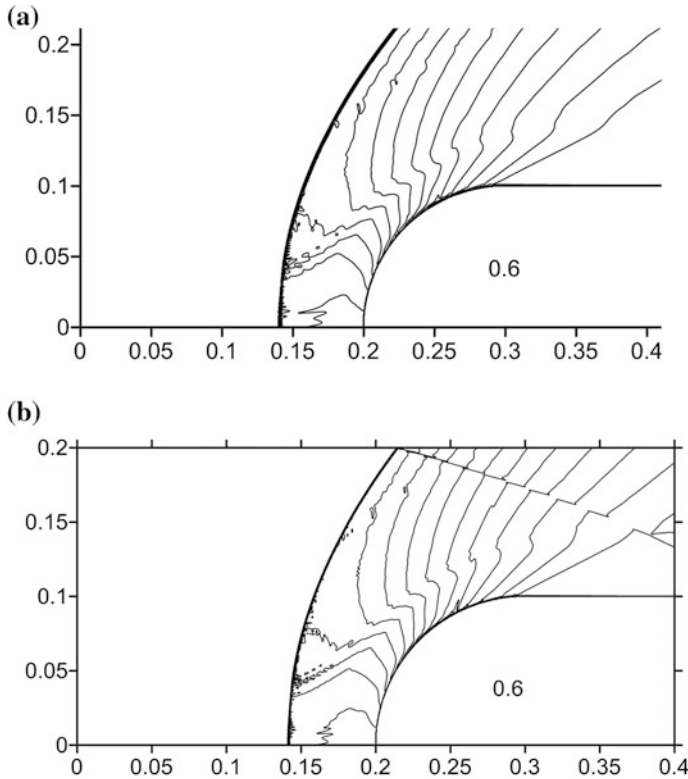


Fig. 11 Steady flow mode for simulations on different calculation areas, $M = 4$, $\gamma = 1.4$: **a** $0 \leq x \leq 0.5$, $0 \leq y \leq 0.5$, $h_x = h_y = 0.0002$ (framed); **b** $0 \leq x \leq 0.2$, $0 \leq y \leq 0.4$, $h_x = h_y = 0.0001$

have calculated the angles through the coordinates of the centers of the triple configurations and the points on the shock fronts in the neighborhood of the center (via the facilities of a graphical editor). The precision is $1\text{--}2^\circ$ for moderate α_p and $3\text{--}4^\circ$ for small α_p .

It should be noted that the boundary conditions can affect the details of forming a triple configuration (see Kemm [20]). To evaluate this influence the additional simulations have been made on the enlarged calculation area: $0 \leq x \leq 0.5$, $0 \leq y \leq 0.5$ (Fig. 11). It can be seen that the fields of the parameters are quite the same for these two calculations. Besides, it was obtained that the maximal difference in the values of the angles is $3\text{--}4^\circ$ (the difference is maximal for the reflected shocks). For example, for $\alpha_p = 0.5$ and $\gamma = 1.4$ the difference in the calculations of the angles was 0.9° for ω_1 , 3.4° for ω_2 , 1° for ω_3 and 2.7° for ω_4 .

3.4 Analysis of Stagnation Pressure and Front Drag Force for Different γ

The dynamics of the stagnation pressure p_t and the front drag force F have been studied in this section (see Fig. 12, subscript “0” is referred to the values of the parameters in the absence of the energy source). The first minimum in the curves is caused by a rarefaction wave reflection which is generated at the very beginning of the interaction process (see Georgievsky and Levin [21]). In Azarova and Knight [22] it has been shown that the next fall down is connected with the action of the vortex structure on the body’s boundary. The drag reduction initiated by a vortex has been obtained numerically in Kolesnichenko et al. [23].

It is seen that the pressure fall down (together with the drag force) at the first stage is greater for smaller γ , but the stagnation pressure fall down has no effect on the decreasing of the drag force. On the contrary, the vortex action at the next stage is significantly large for smaller γ and caused the essential drag force reduction. That is, in the case of smaller γ a new qualitative behavior of the drag force is taken place. Analysis of the stagnation pressure and frontal drag force for γ varying from 1.4 to 1.1 is presented in Table 2.

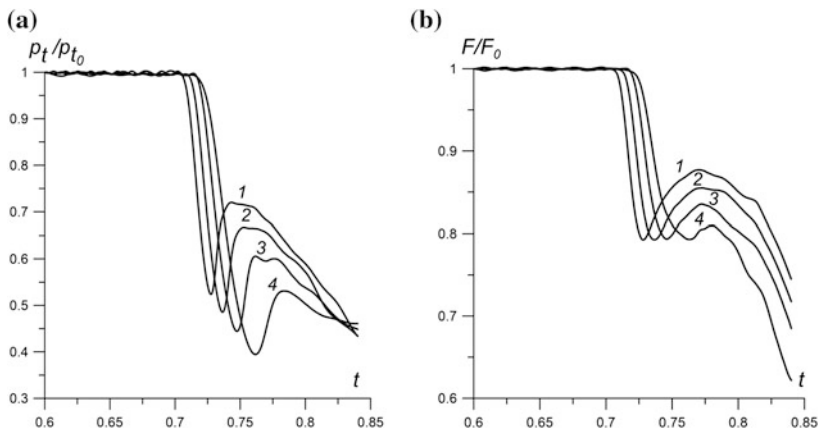


Fig. 12 Dynamics of the related stagnation pressure (left) and front drag force (right) for different γ , $M = 4$, $\alpha_p = 0.5$: curve 1— $\gamma = 1.4$, curve 2— $\gamma = 1.3$, curve 3— $\gamma = 1.2$, curve 4— $\gamma = 1.1$ (Azarova and Gvozdeva [11])

Table 2 Analysis of change of stagnation pressure and frontal drag force with decreasing γ from 1.4 to 1.1

$f(\gamma)$	Related change of f : $[f(1.4) - f(1.1)]/f(1.4)$ (%)	Character of changing $f(\gamma)$ with decreasing γ
$\min(p_t/p_{t0})$	24.7	decreases
$\min(F/F_0)$	16.5	decreases

3.5 Generation of the Richtmyer–Meshkov Instability in the Case of $M = 8$

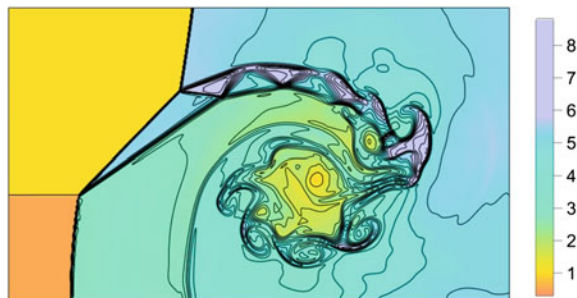
Earlier in Azarova [24], it has been shown that the interaction of a heated channel with a bow shock can give a rise to the Richtmyer–Meshkov instability. Another mechanism of this instability generation is described in this section. Generation of the considered triple-shock configuration is accompanied by forming the vortex structure which includes two contact discontinuities (shear layers) (Fig. 5a). For $M = 8$ and $\gamma = 1.3$ between these contact discontinuities, there arises a flow structure consisting of the rarefaction waves which reflect as the compression waves. This flow structure is similar to that which generates in the shock–shock interaction of “Edney IV” type (see Edney [25]), where the bow shock interacts with the impinging oblique shock. The schematic of the Edney IV shock–shock interaction and a wide review of this subject is presented in Adelgren et al. [26].

The vortex-contact structure obtained here differs from that described earlier by the fact that it is forming as the result of the interaction of the bow shock with two contact discontinuities, which are the boundaries of the heated channel. In the arising vortex-contact structure, the compression waves between shear layers become stronger with increasing freestream Mach number and decreasing γ .

At some time moment, an intersection of the characteristics is taken place causing the “overturn” of the pressure profile in a compression wave and generation of a secondary shock wave. This shock wave interacts with the contact discontinuity which is dislocated under an angle to the shock front being a reason for the Richtmyer–Meshkov instability generation (see Hawley and Zabusky [27]).

This situation has been modeled in the problem of the plane shock wave interacting with the boundary of the heated channel with $\alpha_p = 0.5$ (Fig. 13). One can see the primary vortex generated by the Richtmyer–Meshkov instability (the upper vortex initiated by this instability is suppressed by the high-speed flow) and accompanied by the secondary vortices originated due to the Kelvin–Helmholtz instabilities. Thus, it can be concluded that the generation of the Richtmyer–Meshkov instabilities is typical in such type of problems.

Fig. 13 Generation of Richtmyer–Meshkov instability, density, $M = 8$, $\gamma = 1.3$, $\alpha_p = 0.5$



4 Conclusions

Unsteady Mach triple-shock configurations have been studied at the first stage of the process of interaction of an energy source with a shock layer in the flow mode close to the self-similar one. For freestream Mach number 4, the dependences of the angles of the triple configurations on the ratio of the specific heats γ changing from 1.4 to 1.1 have been studied.

It has been established that with decreasing γ from 1.4 to 1.1 the angle between the reflected shock and the flow direction decreases (by 51.8% for $\alpha_p = 0.5$), the angle of the Mach shock increases (by 11.5% for $\alpha_p = 0.5$), and the angles of the incident shock and of the contact discontinuity are practically independent of γ .

The dependences of the angles of the triple configurations on the rarefaction factor in the energy source α_p , $0.11 < \alpha_p < 0.66$, for γ from 1.4 to 1.1 have been obtained. It has been shown that for all considered γ , the angles of the incident shock and of the contact discontinuity increase against α_p , the angles of the reflected shock have local minima in the interval $0.11 < \alpha_p < 0.66$ and the angles of the Mach shock decrease slightly against α_p .

It has been shown also that with decreasing γ the stagnation pressure fall down caused by the effect of the energy release in the external flow increases by 24.7% and the frontal drag force reduction increases by 16.5% (for $\alpha_p = 0.5$), the latter effect is due to the vortex structure action.

Generation of the Richtmyer–Meshkov instability accompanying the triple-shock configuration has been modeled in the case of $M = 8$. It has been shown that the generation of the Richtmyer–Meshkov instabilities is expected in such types of problems.

Acknowledgements The research is partially supported by RFBR under the Project No. 16-08-01228.

References

1. Bazhenova, T.V., Gvozdeva, L.G., Nettleton, M.A.: Unsteady interactions of shock waves. *Prog. Aerosp. Sci.* **21**, 249–331 (1984)
2. Arutyunyan, G.M., Belokon, V.A., Karchevsky, L.V.: On adiabatic index effect on reflection of shock waves. *J. Appl. Mech. Tech. Phys.* (1), 62–66 (1970) (in Russian)
3. Gvozdeva, L.G., Gavrenkov, S.A., Nesterov, A.A.: Study of slipstreams in triple-shock wave configuration. *Shock Waves* **25**(3), 283–291 (2015)
4. Gvozdeva, L.G., Gavrenkov, S.A.: New configuration of irregular reflection of shock waves. In: Knight, D., Lipatov, I., Reijasse, Ph. (eds.) *Progress in Flight Physics*, vol. 7, pp. 437–452. Torus Press (2015)
5. Georgievsky, P.Y., Levin, V.A.: Front separation flows for blunt and streamlined bodies supported by localized upstream energy deposition. In: *2nd European Conferences of Aerospace Sciences (EUCASS, July 1–6, Brussels)*, pp. 1–8 (2007)
6. Azarova, O.A.: Simulation of stochastic pulsating flows with instabilities using minimum-stencil difference schemes. *J. Comp. Math. Math. Phys.* **49**(8), 1397–1414 (2009)

7. Azarova, O.A., Knight, D.D., Kolesnichenko, Y.F.: Pulsating stochastic flows accompanying microwave filament/ supersonic shock layer interaction. *Shock Waves* **21**(5), 439–450 (2011)
8. Knight, D.: Survey of aerodynamic drag reduction at high speed by energy deposition. *J. Propul. Power* **24**, 1153–1167 (2008)
9. Knight D.: A short review of microwave and laser discharges for supersonic flow control. *J. AerospaceLab* (10), 1–12 (2015)
10. Russell, A., Zare-Behtash, H., Kontis, K.: Joule heating flow control methods for high-speed flows. *J. Electrost.* (4), 1–90 (2016)
11. Azarova, O.A., Gvozdeva, L.G.: Unsteady triple configurations and vortex-contact structures initiated by interaction of an energy source with a shock layer in gases. *Tech. Phys. Lett.* **42** (8), 799–803 (2016)
12. Artem'ev, V.I., Bergel'son, V.I., Nemchinov, I.V., Orlova, T.I., Smirnov, V.A., Hazins, V. M.: Changing the regime of supersonic streamlining obstacle via arising the thin channel of low density. *Fluid Dyn.* (5), 146–151 (1989) (in Russian)
13. Azarova, O.A.: Complex conservative difference schemes for computing supersonic flows past simple aerodynamic forms. *J. Comp. Math. Math. Phys.* **55**(12), 2025–2049 (2015)
14. Grudnitsky, V.G., Prohorchuk, Y.A.: An approach of construction of difference schemes with arbitrary order of approximation of differential equations in partial derivatives. *Reports of RAS* **234**(6), 1249–1252 (1977) (in Russian)
15. Belotserkovsky, O.M., Grudnitsky, V.G., Prohorchuk, Y.A.: Difference scheme of the second order accuracy on a minimal stencil for hyperbolic equations. *J. Comp. Math. Math. Phys.* **23** (1), 119–126 (1983) (in Russian)
16. Semenov, A.N., Syschikova, M.P., Berezkina, M.K.: Experimental study of the specific features of the Mach reflection in a shock tube. *J. Tech. Phys.* **15**(5), 795–803 (1970) (in Russian)
17. Bazhenova, T.V., Gvozdeva, L.G., Lagutov, Y.P., Lyakhov, V.N., Poresov, Y.M., Fokeev, V. P.: *Unsteady Interaction of Shock and Detonation Waves in Gases*, 208 p. Nauka, Moscow (1986) (in Russian)
18. Gvozdeva, L.G., Borsch V.L., Gavrenkov, S.A.: Analytical and numerical study of three shock configurations with negative reflection angle. In: Kontis, K. (ed) 28th International Symposium on Shock Waves, vol. 2, pp. 587–592. Springer (2012)
19. Azarova, O.A.: Complex conservative difference schemes in modeling of instabilities and contact structures. In: Kontis, K. (ed) 28th International Symposium on Shock Waves, vol. 2, pp. 683–689. Springer (2012)
20. Kemm, F.: On the proper setup of the double mach reflection as a test case for the resolution of gas dynamics codes. *Comput. Fluids* (4), 1–7 (2014)
21. Georgievsky, P.Y., Levin, V.A.: Unsteady interaction of a sphere with atmospheric temperature inhomogeneity at supersonic speed. *Fluid Dyn.* **28**(4), 568–574 (1993)
22. Azarova, O.A., Knight, D.D.: Interaction of microwave and laser discharge resulting “heat spots” with supersonic combined cylinder bodies. *Aerosp. Sci. Technol.* (43), 343–349 (2015)
23. Kolesnichenko, Y.F., Brovkin, V.G., Azarova, O.A., Grudnitsky, V.G., Lashkov, V.A., Mashek, I.C.: Microwave energy release regimes for drag reduction in supersonic flows. *Paper AIAA-2002-0353*, 1–12 (2002)
24. Azarova, O.A.: Generation of Richtmyer-Meshkov and secondary instabilities during the interaction of an energy release with a cylinder shock layer. *Aerosp. Sci. Technol.* (42), 376–383 (2015)
25. Edney, B.: Anomalous heat transfer and pressure distributions on blunt bodies at hypersonic speeds in the presence of an impinging shock. *Aeronautical Research Institutes of Sweden, FAA Rept. 115*, Stockholm (1968)
26. Adelgren, R.G., Yan, H., Elliott, G.S., Knight, D.D., Beutner, T.J., Zheltovodov, A.A.: Control of Edney IV interaction by pulsed laser energy deposition. *AIAA J.* **43**(2), 256–269 (2005)
27. Hawley, J.P., Zabusky, N.J.: Vortex paradigm for shock-accelerated density-stratified interfaces. *Phys. Rev. Lett.* No. **63**, 1241–1244 (1989)